Hindawi
Advances in Materials Science and Engineering
Volume 2023, Article ID 3517521, 16 pages
https://doi.org/10.1155/2023/3517521

Research Article

The Characterisation of Fracture Resistance of Asphalt Mixtures Containing Rubber Modifiers and a Wax-Based Additive

Sharvin Poovaneshvaran,[1] Mohd Rosli Mohd Hasan,[1] Ali Jamshidi,[2] Mohd Fahmi Haikal Mohd Ghazali,[1] Xu Yang,[3] and Ramadhansyah Putra Jaya[4]

[1]*School of Civil Engineering, Universiti Sains Malaysia, Engineering Campus, Nibong Tebal 14300, Penang, Malaysia*
[2]*School of Science, Technology and Engineering, University of the Sunshine Coast, Sippy Downs, Queensland, Australia*
[3]*School of Highway, Chang'an University, Xi'an 710064, China*
[4]*Faculty of Civil Engineering Technology, Universiti Malaysia Pahang, Kuantan 26300, Pahang, Malaysia*

Correspondence should be addressed to Mohd Rosli Mohd Hasan; cerosli@usm.my

Received 18 October 2022; Revised 6 January 2023; Accepted 7 January 2023; Published 17 January 2023

Academic Editor: Chenggao Li

Asphalt mixture modification with rubberised material frequently results in improved characteristics and extended service life in actual application. This research characterised the synergistic consequences of rubber modifiers (crumb rubber powder (CRP) and natural rubber latex (NRL)) and wax-based admixtures (Tough Fix Hyper (TFH)) on the performance of the asphalt mixture from the fracture energy and laboratory fracture resistance perspectives. Semicircular bending (SCB) and indirect tensile strength (ITS) tests were conducted to assess the fracture properties of the asphalt mixture samples. To prepare asphalt mixture samples, the wet method was utilised. Higher CRP levels resulted in greater strength and a longer time to attain peak force for both control and mixtures containing wax admixture, as determined by SCB. The interaction between the higher CRP or NRL content and the TFH additive enhanced the fracture resistance, indicating that the components are highly compatible. The 10L + TFH additive produced the highest fraction of energy, indicating a more significant improvement than the counterpart mixes containing the CRP modifier. In addition, incorporation of the CRP and NRL increased the fracture plastic zone (FPZ), resulting in increased fracture toughness. Therefore, the gradient of fracture toughness and fracture energy in the asphalt mix depends on the rubber type, content, and TFH. Although the higher CRP, NRL, and TFH improve the fracture energy and cracking resistance, they increase the crack initiation and propagation velocities, whereby the high bitumen stiffness makes the mixture more brittle than the control mixture. Caution should be exercised when selecting the content of rubber modifier and TFH for the asphalt pavements in low-temperature service. Also, there is a direct interconnection between fracture resistance and fracture energy in the mixtures containing CRP, NRL, and TFH. Such correlations can be used as the premise of predictive micro- and macro-models to evaluate mixture performance in terms of fracture resistance.

1. Introduction

Previous research has shown that the implementation of recycled crumb rubber and natural rubber latex biopolymer as asphalt modifiers improves the performance of road surfacing materials [1–4].Rubber-modified asphalt mixture has superior resistance to rutting, thermal cracking, fatigue damage, and stripping and lower temperature sensitivity [5–7]. Compared to the conventional asphalt binder, using natural or synthetic polymers has significantly enhanced the binder properties [8, 9]. By enhancing the serviceability of the pavement, this approach has benefited the paving industry and provided forgiving road conditions for road users.

The fracture distress of asphalt mixtures is an important factor in determining the serviceability of flexible pavements. The fracture decreases the pavement's functional performance, eventually leading to structural failures. Subsequently, further costs for maintenance and rehabilitation would be incurred [10]. Therefore, the analysis

of fracture is important to characterise the failure mechanism of the pavement over its life span and to develop models for pavement management services [11–13].

If the flexural and shear stress/strain exceeds the resistance of the mixture components, cracking is inevitable in three modes at the crack tip as shown in Figure 1 [14]. The *x*-axis is perpendicular to the crack front, the *y*-axis being aligned to the crack plane, and the *z*-axis being aligned to the crack front. The fundamental modes of three modes of cracking can be visualised in Figure 2. In the Mode I opening phase, tensile stress/strain results in cracking in the asphalt mixture's matrix. In Mode II, the shear stress flows through the weakened parts of the mix components, which are asphalt and mortar, during the sliding phase. In comparison, a fracture faces coarse aggregate particles in the flow track and the direction of the shear flow changes. In other words, shear stress flows to align with the crack plane and is perpendicular to the crack front. In Mode III, the crack propagation occurs in all three dimensions, as in the tearing phase. In other words, shear stress flows to align with the plane of the fracture and crack front. In Mode III, strain flow and shear stress pass through the weakened zone of an asphalt mixture matrix, similar to Mode II [14, 15]. The weakened zones comprise a film of asphalt binder, mortar, and aggregate particles that are not fully coated by asphalt binder.

To characterise and analyse the fracture in the asphalt mixtures, different methodologies, procedures, and apparatuses were developed. There are also numerous crack propagation micro- and macro-models with various inputs. For example, a laboratory and in-situ research at the University of Florida led to a viscoelastic cracking mechanics-based model based on resting duration, microdamage, dispersion of the crack, and healing for stated loading situations and temperatures [16]. In another laboratory research, Wei et al. [17] analysed the trend of cracking using an image-based numerical approach and acoustic emission. According to the model results, the crack begins as a weakened zone at the aggregate-mortar interface and then disperses slowly parallel to the surface [18]. However, He et al. reported that about 10–15% of the fracture surface of the crack propagation passes, owing to the shattering of the densely packed aggregate particles. This range changes based on the failure mode. For example, Modes II and III have lower percentage drops in loading conditions and elevated testing temperatures. Compared to brittle and isotropic construction materials, asphalt mixtures with coarser aggregate gradation in the ligament exhibit a fracture pattern with significant variation at the midrange temperature [19].

Fracture toughness (K_{IC}) is one of the variables for analysing failure mechanisms; it is the material's resistance to crack propagation [18, 20, 21]. Various experimental procedures existed to estimate the K_{IC} of asphalt mixtures as follows:

(i) Edge cracked rectangular beam loaded with three- or four-point bending [20, 22–24]

(ii) Edge cracked circular compact tension sample by pin loading [22, 25, 26]

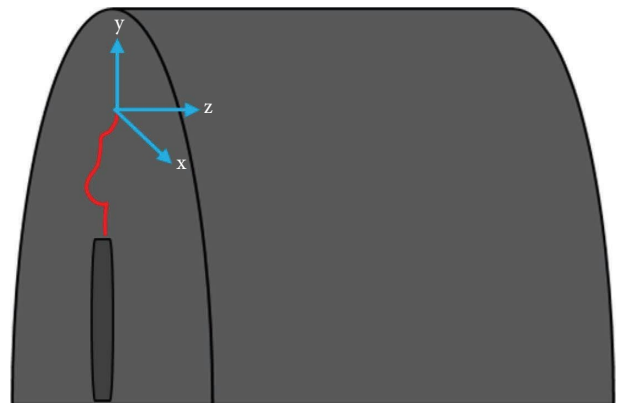

Figure 1: Local coordinate system on a crack tip of fracture asphalt mixture.

(iii) Edge cracked semicircular sample loaded with symmetric three-point bending [27–29]

(iv) Center cracked Brazilian disc sample subjected to the diametral compression loading mode [19, 30]

(v) Edge cracked disc sample subjected to the diametral compression mode [31, 32]

(vi) Edge cracked disc sample subjected to three-point bending [33, 34]

(vii) Edge cracked circular disc loaded with wedge splitting fixture [35]

(viii) Indirect diametral test [36]

Generally, K_{IC} is determined by temperature, loading rate, material, features, and sample geometry [37–39]. Regardless of the test protocols and analytical methods, using different materials and building technologies may affect K_{IC} [40]. For example, Sabahfar et al. [41] evaluated the potential of cracking in the asphalt mixtures that accommodate 20% to 40% reclaimed asphalt pavement (RAP) supplied from different sources using simplified viscoelastic continuum damage (S-VECD) tests, semicircular bending (SCB), dynamic modulus, and Texas overlay. Compared to other approaches, the S-VECD method produced more sensitive responses to changes in RAP content and characteristics. Furthermore, research conducted by Zarei et al. [42] showed that pure Modes I and II can characterise warm-mix asphalt (WMA) fractures. In addition, based on the observation, the distribution of coarse aggregate particles in the specimen's ligament section contributes significantly to the fracture property of the WMA mixture. It should be noted that the reduced stiffness of the mixture results in improved fracture resistance. For instance, Kavussi and Motevalizadeh [43] found that the foam-WMA mixtures with a lower RAP content (up to 50%) have a higher resistance to fracture propagation, which is consistent with the results outlined by Yousefi et al. [44].

Despite the fact that numerous studies on the fracture performance of various types of mixtures have been conducted, there is a scarcity of sound research focusing on the characterization of the interaction between materials and technology used in the production of asphalt mixes on

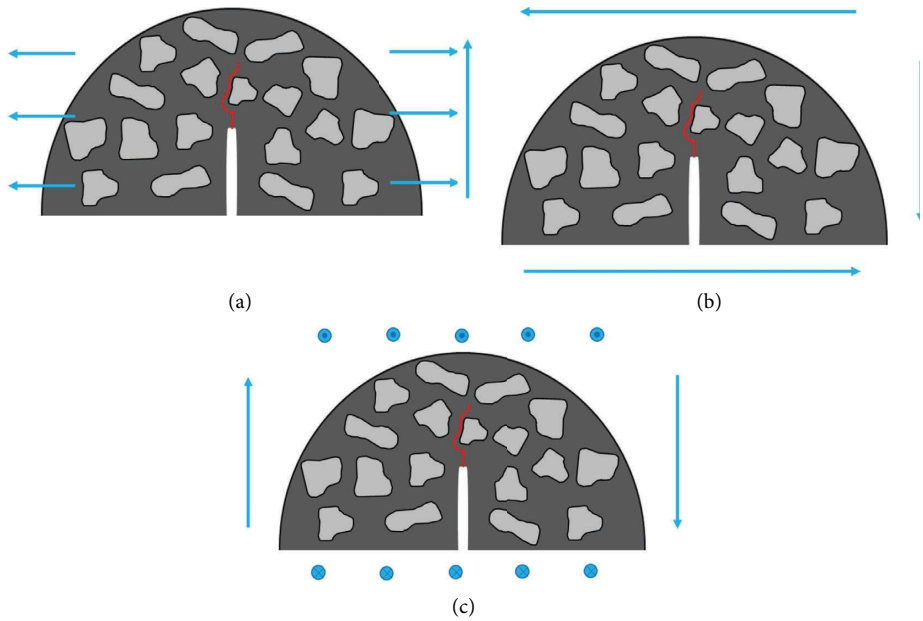

Figure 2: Three modes of cracking of asphalt mixture under flexural load: (a) mode I (tensile on x-axis):opening phase, (b) mode II (shear stress align to crack plane on y-axis and 90° to crack front on x-axis):sliding phase, and (c) mode III (shear stress parallel on crack plane and crack front on y-axis and z-axis):tearing phase.

fracture performance. To fill a knowledge gap, this research investigates the interrelationship between rubber modifiers and surfactant technology on mixture cracking performance using various test procedures. In addition, the test's purpose was to determine the effect of varying modifier concentrations on the cracking performance of asphalt mixtures.

2. Materials and Methods

2.1. Materials

2.1.1. Aggregates. The aggregate used in the preparation of the asphalt mixture samples was granite aggregate supplied by Kuad Quarry Sdn. Bhd., Penang. The aggregate was dried in the oven at 105°C overnight and then sieved using a mechanical shaker. A dense-graded mixture grading that conforms to the Malaysian Public Work Department (PWD) was adopted. The engineering properties of the aggregates are shown in Table 1.

2.1.2. Asphalt Binder. As the base binder, a 60/70 penetration grade binder was utilised. Table 2 summarises the asphalt binder's properties.

2.1.3. Crumb Rubber Powder. The origin of crumb rubber powder (CRP) was basically produced from scrap tires. The acquired CRP was sieved to determine the distribution of particle size. Table 3 shows the CRP gradation. In order to retain the reliability and quality of the CRP, a single batch of the crumb rubber powder produced by a local supplier was used throughout this research.

The existing crystalline phase and mineralogical composition of the CRP were determined using X-ray diffraction (XRD) test. Table 4 presents the XRD result.

2.1.4. Natural Rubber Latex. The natural rubber latex (NRL) obtained from a local vendor was used for this research. Basically, rubber hydrocarbon and nonrubber material are the two primary components of NRL. It has distinct chemical and physical characteristics that are considerably affected by the presence of the nonrubber constituent. The physical and chemical properties of NRL must be maintained to certify the quality of the latex used for asphalt binder modification. Table 5 summarises the NRL properties.

2.1.5. Wax-Based Additive. In this research, a wax-based additive was utilised to improve the bonding characteristics in the rubberised asphalt mixture. The dosage of additive used in this research is 0.15% by the mass of the asphalt binder. The properties of wax-based additive are summarised in Table 6.

2.1.6. Modified Asphalt Binders. Prior to the preparation of the mixture samples, the CRP- and NRL-modified asphalt binders with 0.15% TFH by mass of bitumen were blended in batches. The CRP and NRL of 5% and 10% were used for modification purposes. The asphalt binder was preheated in an oven at 160°C for two hours, and a thermo-cell monitored the exact temperature during the blending process. A propeller mixer was used for the blending process, and the

Table 1: Physical properties of granite aggregates.

Physical properties	Result	Specification	Test method
Coarse aggregates bulk specific gravity	2.67	—	AASHTO T85
Coarse aggregates absorption	0.40	<2%	AASHTO T85
Fine aggregates bulk specific gravity	2.60	—	AASHTO T84
Fine aggregates absorption	0.31	<2%	AASHTO T84
Aggregates crushing value	19.75	<25%	ASTM C131
Los Angeles abrasion	21.25	<25%	ASTM C131
Flakiness index	18.77	<25%	BS EN 933-3
Elongation index	19.76	<25%	BS EN 933-3

Table 2: Properties of asphalt binder.

Properties	Value	Test method
Viscosity @ 135°C, (mPa·s)	575	AASHTO T 316
$G^*/\sin\delta$ @ 10 rad/s (unaged), (kPa)	1.04	
$G^*/\sin\delta$ @ 10 rad/s (short-term aged), (kPa)	2.23	AASHTO T315
$G^*.\sin\delta$ @ 10 rad/s (long-term aged), (kPa)	4550	
Relative density	1.03	ASTM D70
Softening point, °C	50	ASTM D36
Penetration @ 25°C, (dmm)	66	ASTM D5
Ductility @ 25°C, (cm)	>100	ASTM D113

Table 3: Crumb rubber powder gradation.

Sieve size (mm)	% passing
20	100
14	100
10	100
5	100
3.35	100
1.18	100
0.425	50
0.15	9
0.075	1
Pan	0

Table 4: Mineralogy compounds of crumb rubber powder.

Mineralogy compounds	Symbols	Percentage (%)
Carbon	C	87.44
Aluminium	Al	0.1
Oxygen	O	9.01
Zinc	Zn	2.05
Silicon	Si	0.32
Magnesium	Mg	0.11
Sulphur	S	0.97

Table 5: Properties of NRL.

Parameters	Description
Form	Liquid
Colour	Milky white
pH	10.00
Total solids content (TSC)	58%
Dry rubber content (DRC)	60.1%
Mechanical stability time (MST)	720 s
Viscosity @ 100 rpm	163.2 cP
Alkalinity with cationic stabilizer	0.35
Alkalinity with nonionic stabilizer	0.32
Alkalinity with anionic stabilizer	0.40
Potassium hydroxide (KOH) number	0.97
Volatile fatty acid (VFA) number	0.18

Table 6: Properties of the TFH wax-based additive.

Properties	Value
Melting point using ascending method	125°C
Viscosity @ 140°C	393 MPa·s
Viscosity @ 160°C	165 MPa·s
pH with 1% concentration of water	9.6
Flash point by Cleveland open cup	286°C

modifiers asphalt binder was blended for 30 minutes. The sample designation and types of asphalt mixtures assessed are summarised in Table 7. Figure 3 shows the physical appearance of modifiers and additives used in this research.

2.2. Experimental Methods

2.2.1. Fracture Behaviour Assessment via Semicircular Bending (SCB) Test. The SCB test was used to examine the fracture properties of the asphalt mixture following AASHTO TP105. The specimen is prepared with a 15 mm notch depth and in the form of a half-disc. Formerly, the specimens were compacted to a thickness of 50 mm and a diameter of 150 mm. Before the SCB test, the specimens were preconditioned at 10°C for 4 hours. The maximum loading achieved and the deformation of the specimens were monitored. This test method evaluates the fracture energy (G_f) of the asphalt mixtures.

Table 7: Sample designation and types of asphalt binder.

Sample no.	Sample designation	*Compositions*					
		60/70	5% CRP	10% CRP	5% NRL	10% NRL	TFH
1	CB	Y	X	X	X	X	X
2	CB + TFH	Y	X	X	X	X	Y
3	5CR	Y	Y	X	X	X	X
4	5CR + TFH	Y	Y	X	X	X	Y
5	10CR	Y	X	Y	X	X	X
6	10CR + TFH	Y	X	Y	X	X	Y
7	5L	Y	X	X	Y	X	X
8	5L + TFH	Y	X	X	Y	X	Y
9	10L	Y	X	X	X	Y	X
10	10L + TFH	Y	X	X	X	Y	Y

Y = include and X = does not include.

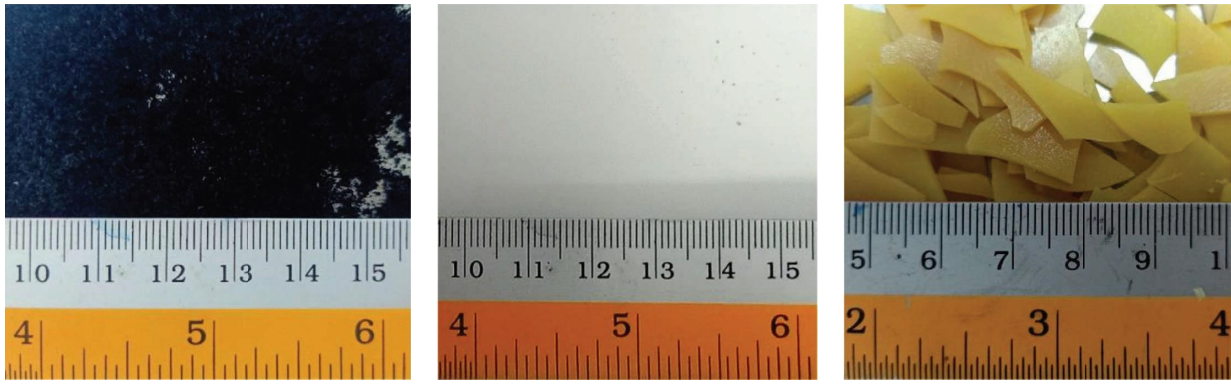

(a) (b) (c)

Figure 3: Physical appearance of the modifiers and additive used: (a) crumb rubber powder, (b) natural rubber latex, and (c) wax-based additive.

Besides, this approach includes the procedures for calculating K_{IC} and stiffness (S). In addition, new fracture initiation and crack development rate parameters based on previous studies were also assessed. All the stated parameters above can be calculated using Equations (1) to (8).

(1) Calculation of fracture energy

$$\text{Fracture Energy}, G_f = \frac{W_f}{A_{\text{lig}}}, \tag{1}$$

where G_f = the fracture energy (J/m^2); W_f = the work of fracture (J), where W_f is $\int$Pdu; P = the applied load (N); u = the average load line displacement (m); Alig = the ligament area (m^2), where A_{lig} is (r − a) × t; r = the specimen radius (m); a = the notch length (m); and t = the specimen thickness (m)

The total work of fracture is then calculated as the sum of W and W_{tail}:

$$W_f = W + W_{\text{tail}}, \tag{2}$$

$$W = \text{area} = \sum_{i=1}^{n} \left(u_{i+1} - u_i\right) \cdot \left(P_i\right) + \frac{1}{2} \cdot \left(u_{i+1} - u_i\right) \cdot \left(P_{i+1} - P_i\right), \tag{3}$$

where P_i = the applied load (N) at the i load step application; P_{i+1} = the applied load (N) at the i+1 load step application; u_i = the average LLD load line displacement (m) at the i step; and u_{i+1} = the average LLD load line displacement (m) at the i + 1 step:

$$W_{\text{tail}} = \int_{u_c}^{\infty} Pd(u) = \int_{u_c}^{\infty} \frac{c}{u^2} d(u) = \frac{c}{u_c}, \quad (4)$$

where u = the integration variable equals to average load line displacement (m) and u_c = the average load line displacement value at which the test stops (m).

(2) Calculation of fracture toughness

At the critical load, P_c, the fracture toughness, K_{IC}, is obtained from the stress intensity factor, K_I. It is presumed that the maximum load measured during testing represents the critical load. The stress intensity factor, K_I, is calculated using the following equation:

$$\frac{K}{\sigma_0 \sqrt{\pi a}} = Y_{I(0.8)}, \quad (5)$$

where σ_0 = P/2rt; P = the applied load (MN); r = the specimen radius (m); t = the specimen thickness (m); a = the notch length (m); and Y_I = the normalised stress intensity factor (dimensionless).

For the dimensionless SCB specimens used in this test method, Y_I is calculated using the following equation:

$$Y_{I(0.8)} = 4.782 + 1.219\left(\frac{a}{r}\right) + 0.063e^{(7.045(a/r))}. \quad (6)$$

(3) Calculation of stiffness

The stiffness S is computed using the slope of the linear component of the ascending load-average load line displacement curve.

(4) Calculation of fracture initiation velocity

$$v_{FI} = \frac{\int_0^{\text{peakload}} Pdu}{t_{\text{peakload}} - t_0} = \frac{G_{f\text{peakload}} - G_{f0}}{t_{\text{peakload}} - t_0} = \frac{\cdot G_f}{\cdot t}, \quad (7)$$

where V_{FI} = the velocity of fracture initiation (J/m^{2}s); P = the load; $G_{\text{fpeakand0}}$ = the fracture energy at peak and test initiation (J/m^2); and t = the elapsed time.

(5) Calculation of crack growth velocity

$$v_{CG} = \left|\frac{F_{\text{end}} - F_{\max}}{t_{\text{end}} - t_{\max}}\right| = \left|\frac{\cdot F}{\cdot t}\right| = \left|\frac{\partial F}{\partial t}\right|, \quad (8)$$

where V_{CG} = the absolute value of the slope of the descending linear part of load versus elapsed time curve which indicates the velocity of crack growth (kN/s); ΔF = the load decrement (kN) from the peak to the total failure occurrence; and Δt = elapsed time from peak to the end.

2.2.2. Indirect Tensile Strength Test. In conjunction with laboratory mix design testing, indirect tensile strength (ITS) values can be used to evaluate the relative quality of asphalt mixtures and their resistance to rutting or cracking. A high tensile strain of a specimen at failure signifies that it can endure a higher strain before failing and is more resistant to cracking. Conforming to ASTM D693, the ITS test was conducted, and the specimens were stored at 15°C for four hours before testing. The ITS values of the specimens were calculated and analysed using equation (9):

$$ITS = \frac{2P_{\max}}{\pi t d}, \quad (9)$$

where $P_{\max}$ = the maximum applied load in N; t = the height of specimen in mm; and d = the diameter of specimen in mm.

3. Results and Discussion

3.1. Fracture Resistance via Semicircular Bend (SCB) Geometry. Only the Mode I loading condition has been adopted for assessment in this research. As a consequence of thermal stresses, the Mode I loading condition belongs to tension (bending). After the loading period, all the asphalt mixture samples were subjected to a validation test to ensure that crack propagation occurs within 10% of the specimen's diameter from the loading strip's centre. Figure 4 shows the validation test.

The 3D surface plots shown in Figures 5(a)–5(d) were used to investigate the correlation between a response variable (force) and two predictor variables (modifier content and time taken to reach peak load). The plot shows the impact of modifier concentration on the force and time required to reach peak load. The force presented in these 3D surface plots corresponds to the peak load obtained directly from the load versus displacement curve. From the 3D surface plot, the modified asphalt mixture can sustain a more significant load, so it takes longer to achieve peak load before

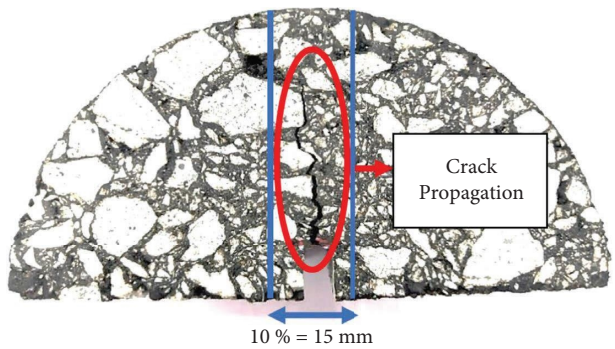

Figure 4: Validation test of asphalt mixture's crack propagation.

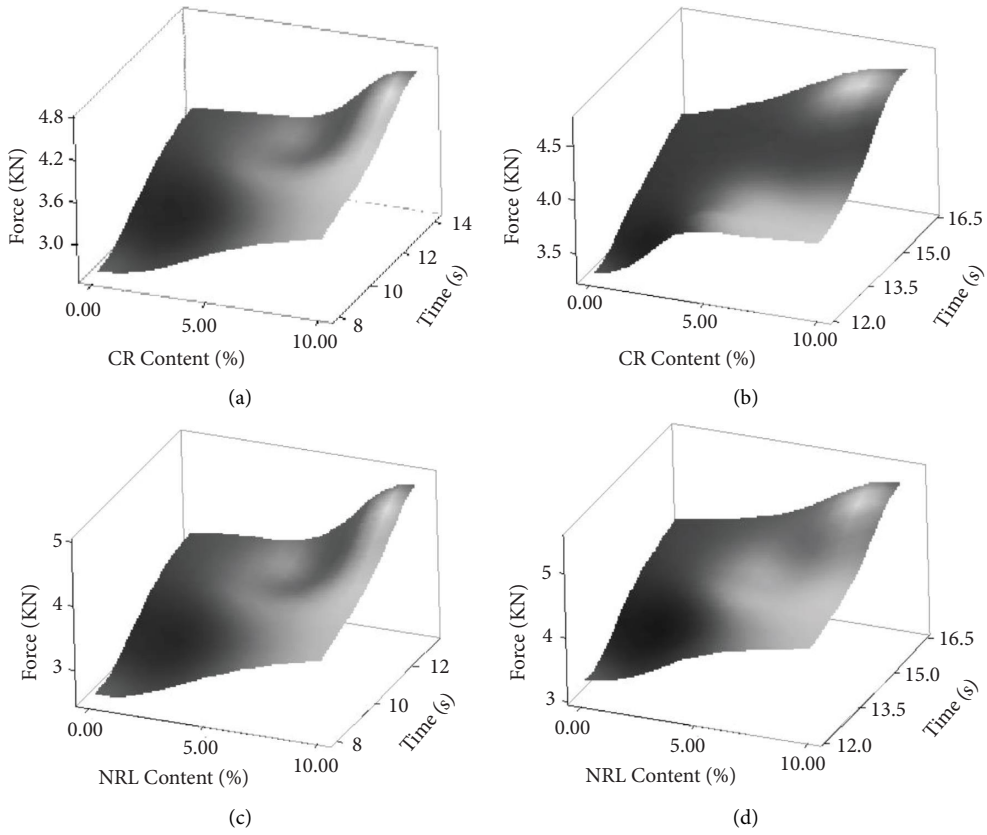

Figure 5: Surface plot of asphalt mixtures on effects of modifier content on the force and duration taken to reach the peak load: (a) CRP-modified asphalt mixture without TFH, (b) CRP-modified asphalt mixture with TFH, (c) NRL-modified asphalt mixture without TFH, and (d) NRL-modified asphalt mixture with TFH.

failing. Also, this shows that the respective modified asphalt mixture sample could sustain the applied load for an extended time before reaching its maximum load and failing. The peak of each 3D surface plot reveals the best performance of the asphalt mixture. All the modified asphalt mixtures, including those containing 10% rubber modifiers, achieved the highest position on the 3D surface plot compared to the control asphalt mixture. The incorporation of TFH and higher percentages of rubber modifiers enhanced the performance of the asphalt mixture by achieving a higher load. The higher force and longer duration ascribed to the higher modifier content reveal that the sample shows a sign of better fracture resistance in comparison to an asphalt mixture prepared without modifiers and TFH. Even though all the results have a similar trend, the maximum force obtained from the load against the displacement curve needs to be more persuasive to be used as an indicator of fracture resistance because the calculated maximum force does not account for the geometry of asphalt mixtures.

3.1.1. Fracture Energy of Asphalt Mixtures (G_f). Instead of utilising the force computed directly from the load-displacement curve, the asphalt mixture fracture properties are easily explained by the fracture energy (G_f) approach through linear elastic fracture mechanics (LEFM). To calculate the fracture energy using the LEFM method, it is necessary to account for the area below the curve of the load-displacement graph. Fracture energy signifies the external energy needed for a crack to evolve. The fracture energy is used as a metric to distinguish asphalt mixtures with improved crack resistance. It is also the fundamental metric employed in more sophisticated investigations involving the fictitious fracture (cohesive zone). Figure 6 illustrates the fracture energies of every asphalt mixture.

Figure 6 demonstrates that the modified CRP- and NRL-based asphalt mixture exhibited higher fracture energy. Higher fracture energy requires more energy to generate a crack surface area. Higher fracture energy is observed in an asphalt mixture prepared with a stiffer asphalt binder. The fracture energy of the control asphalt mixture is observed at the lowest value of 788.73 J/m^2, indicating that the fracture resistance is very low during the crack propagation phase due to the softer asphalt binder. The fundamental principle of the fracture mechanism is that cracking occurs only in the area of the crack tip (notch tip) if the energy accumulated exceeds the fracture energy. The addition of TFH and the higher content of rubber modifiers resulted in a higher fracture energy value. As can be seen, the 10L + TFH has the best resistance against fracture, with the highest fracture energy of 2939.95 J/m^2, which is 3.75 times greater than the control mixture (CB). Figure 6 also depicts the effect of CRP or NRL content on the G_f. For example, the G_f of a mixture containing 10L + TFH is 750 J/m^2, which is higher than the G_f of a mixture containing 5L + TFH, indicating that more than 5% NRL resulted in an extra 750 J/m^2 in G_f. Another example is that the mixture containing 5% CRP and TFH (5CR + TFH) has 200 J/m^2 G_f less than the counterpart mix containing 10% CRP. In other words, an extra 5% of NRL resulted in 750 J/m^2, while the extra 5% of CRP led to 200 J/m^2, indicating that the NRL outperforms CRP in increasing G_f. As a result of this interaction, higher percentages of NRL and TFH can result in a higher G_f compared to CRP and TFH.

3.1.2. Fracture Toughness (KIC) of Asphalt Mixtures. Figure 7 indicates various asphalt mixtures with their respective fracture toughness (K_{IC}). The fracture toughness of asphalt mixtures with enhanced cracking resistance was also used as an index factor. Fracture toughness can be referred to as the stress intensity factor. It is highly dependent on the asphalt mixture geometry. The stress intensity factor will reach its maximum value and cause crack propagation, causing failure to initiate at the notch tip. The asphalt mixture's fracture toughness can be calculated using the LEFM-developed equation. As expected, fracture toughness has a similar trend to fracture energy. The properties of the asphalt mix incorporated with the modified asphalt binders have improved its fracture toughness. The reduced fracture toughness of an asphalt mixture results in crack propagation being perpendicular to the substantial tensile stress in the applied load direction. The fracture toughness increases when a higher concentration of rubber modifiers and TFH is applied. The control asphalt mixture demonstrated more brittle behaviour with a low fracture toughness value. This verifies that the addition of rubber modifiers and TFH improves the cracking resistance at low temperatures.

According to LEFM, crack initiation begins with the fracture plastic zone (FPZ) in the region of the weak zone (notch tip), which is mainly caused by plastic deformation in the material [45]. The FPZ for an elastic material is typically microscale and has a minor impact on the process of fracture analysis. However, the LEFM is used in this case because the asphalt mixture behaves as a quasi-brittle viscoelastic material and the higher magnitude of FPZ causes the fracture process [46]. Enhanced fracture toughness can reduce the occurrence of strain hardening, microcrack growth, and high scale yielding near the crack tip (notch tip) in order to resist cracking. The viscosity of the CRP- and NRL-modified asphalt mixtures is higher, resulting in a greater FPZ at the notch tip. This process contributes to a stress-relieving phenomenon. The higher FPZ helps in managing effective stress at the notch tip by viscoelastic stress relaxation and consequently exhibits superior fracture resistance [46]. A higher FPZ results in higher fracture energy to maintain continuous crack development activity, whereas the control asphalt mixture's viscosity is constrained to create a higher FPZ. Therefore, the control asphalt mixture has a very low fracture toughness value (0.394 MPa $\times$ m$^{0.5}$).

3.1.3. Stiffness of Asphalt Mixtures. The asphalt mixture's stiffness (S) is presented in Figure 8. Using the gradient at the linear portion of the increasing load-displacement curve, the asphalt mixture's stiffness is calculated. The stiffness demonstrated a correlation with the elastic modulus of the asphalt mixture at lowered temperatures. As it is strongly related to pavement distress, such as fatigue and low-temperature cracking, the elastic modulus is a crucial design parameter for pavement structures. The elastic modulus of an asphalt mixture is not a measure of its strength but rather its behaviour.

Fundamentally, temperature changes significantly impact the elastic modulus of the asphalt mixture. However, in this case, various types of asphalt mixtures would be evaluated at the same temperature. According to the findings, adding rubber modifiers and TFH significantly improved the elastic modulus of the asphalt mixture. This finding is consistent with the rheological properties of asphalt binder (complex shear modulus, phase angle, and viscosity), which are rapidly changed by rubber modifiers and the additive. The addition of TFH results in a slight decrease in stiffness in the CB + TFH and 10L + TFH samples. However, the general trend shows that the modification process improved the stiffness of all asphalt mixtures, and the stiffness values are comparable with no significant differences. However, the maximum stiffness values for the NRL-modified asphalt mixtures without and with TFH were 4.57 kN/mm and 4.50 kN/mm, respectively.

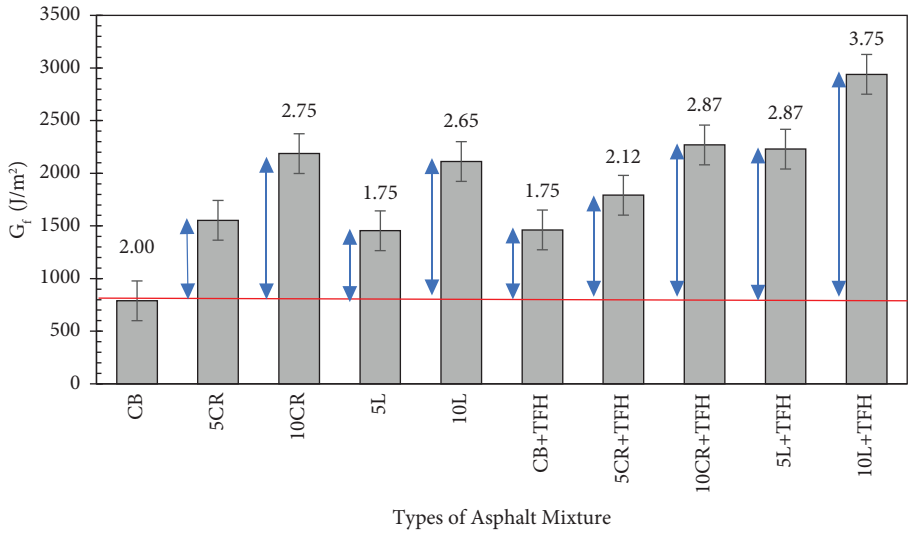

Figure 6: Fracture energy of various asphalt mixtures with percentage difference compared to the control binder.

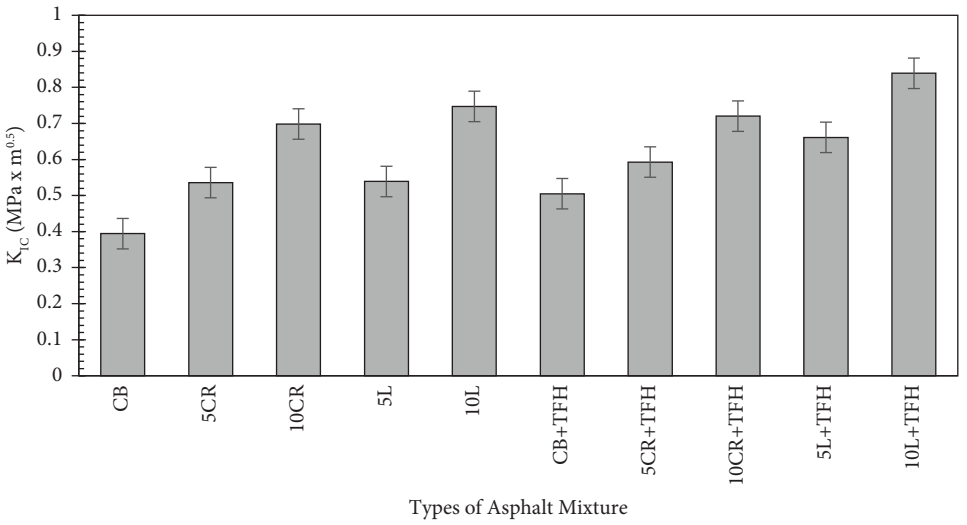

Figure 7: Fracture toughness of various asphalt mixtures.

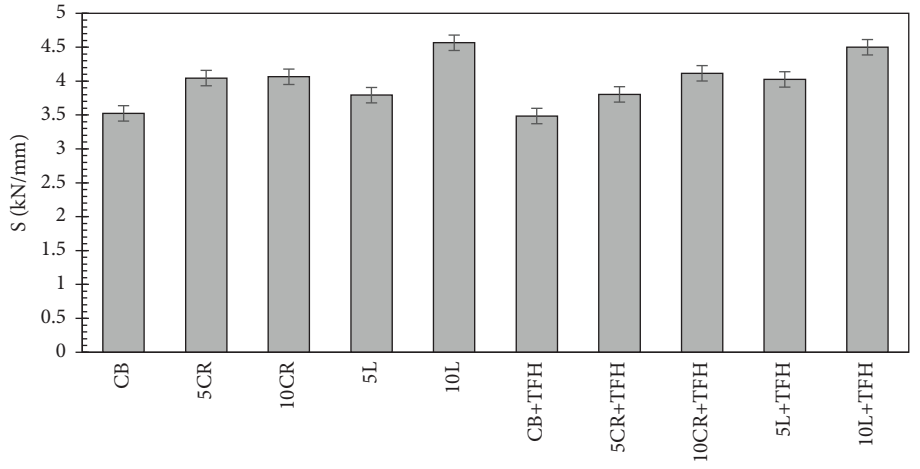

Figure 8: Stiffness of various asphalt mixtures.

A higher elastic modulus implies that the asphalt mixture is resistant to elastic deformation under force application, indicating the viscoelastic behaviour of rubber-modified asphalt binder. As expected, the control asphalt mixture exhibited the lowest stiffness with 3.52 kN/mm and 3.48 kN/mm, without and with TFH, respectively. It must be noted that the elastic range of the asphalt mixture is obtained from the ascending linear part of the load-displacement curve. In this curve region, if the asphalt mixture sample is loaded with any force, it will return to its previous shape and no crack will form. However, once the asphalt mixture reaches the limit of its elastic range, cracks will begin to develop, indicating that it has reached its failure stage. Therefore, the rubber-modified asphalt mixture demonstrated higher loading resistance without immediate cracking and exhibited higher fatigue and low-temperature cracking resistance compared to the control asphalt mixture.

3.1.4. Velocity of Fracture Initiation (VFI) and Crack Growth (VCG) of Asphalt Mixtures. The results tabulated in Table 8 show the fracture initiation and crack growth velocities. Several parameters, such as the fracture behaviour of the asphalt mixture, have been previously discussed. Numerous studies have proposed alternative methods for assessing cracking behaviour, such as fracture initiation and crack growth velocity [37]. The velocity of fracture initiation (V_{FI}) is the rate at which a crack initiates upon reaching its failure limit. While the velocity of crack growth (V_{CG}) refers to the velocity of the crack after its initiation, the crack growth velocity is obtained from the linear gradient of the descending part of the load-displacement curve. The steeper slope would result in a higher velocity value. The outcome indicates that the asphalt mixture prepared with a modified asphalt binder (stiffer asphalt binder) has higher V_{FI} and V_{CG} compared to the asphalt mixture prepared using a control asphalt binder (softer asphalt binder). Despite the fact that there is a slight decrease in V_{FI} and V_{CG} in some instances, the general trend indicates that the increment in rubber modifier percentages and the addition of TFH result in increased V_{FI} and V_{CG}.

Compared to the CRP-modified asphalt mixture, the NRL-modified asphalt mixture has the highest V_{FI} and V_{CG}. Yet, both the NRL- and CRP-modified asphalt mixtures outperform the control asphalt mixture. These results may contradict other parameters, such as fracture energy, fracture toughness, and stiffness, which show that asphalt mixtures made with modified asphalt binders have superior fracture resistance. The higher the stiffness of the modified asphalt binder in nature, the greater the brittleness at low temperatures. Therefore, the increased V_{FI} and V_{CG} are associated with the brittleness of modified asphalt binder due to the low temperature. It can be concluded that higher energy is needed to initiate a crack in the modified asphalt mixture; nevertheless, once the threshold of load-bearing is exceeded, the fracture initiation and crack growth velocity are rapid due to the brittleness of the material. This is due to the elastic energy stored in the specimen during the loading phase, and the rubber-modified asphalt mastic exhibits a ductile failure [47].

Table 8: Velocity of fracture initiation and crack growth of various asphalt mixtures.

Types of asphalt mixture	Velocity of fracture initiation, V_{FI} (J/m^{2}s)	Velocity of crack growth, V_{CG} (kN/s)
CB	98.51	2.87
CB + TFH	120.80	2.21
5CR	122.60	2.81
5CR + TFH	141.93	2.98
10CR	155.45	3.65
10CR + TFH	142.24	3.74
5L	122.98	3.03
5L + TFH	157.17	2.78
10L	160.91	4.55
10L + TFH	182.49	3.85

3.1.5. Analysis of Variance of the SCB Test Results. Statistical analysis was conducted to validate the obtained results of fracture energy and verify the contribution of the CRP modifier, the NRL modifier, and the TFH additive towards the fracture properties of the asphalt mixture. The effect of different factors on the fracture energy of asphalt mixtures was evaluated by conducting an ANOVA and using the general linear model. The results are shown in Table 9. The effect of the selected factors on the fracture behaviour of the asphalt mixture is considered significant if the P-value is <0.05. In addition to evaluating each individual factor, the interaction between the modifier and TFH was also evaluated.

Referring to the variance analysis, it can be summarised that all of the listed factors are statistically significant and contributed to the fracture energy, as their P values are below 0.05. However, the interaction factor between rubber modifiers and TFH does not significantly change the asphalt mixture's fracture properties. It is concluded that different modifier contents and types, as well as the addition of TFH, increased the crack resistance of the asphalt mixtures. The percentage of contributions is based on the estimates of the variance components, reflecting the degree of effect on the crack resistance properties. Therefore, as shown in Table 9, 52.08% of the total variation in the measurements is due to the NRL content. It is evident from the results that the inclusion of the NRL modifier at various percentages significantly enhanced the crack resistance properties. The percentages of contribution for CRP contents and the wax-based additive are 9.10% and 17.91%, respectively. The contribution due to the interaction between modifier content and TFH can be assumed to be less significant. Figure 9 shows the normal plots of residuals. The normal probability plot of residuals is used to verify that residuals have a normal distribution. The general linear model can evaluate the impact of various factors on the response of results based on the normal distribution of residuals along the fitting line.

Table 9: ANOVA data of fracture energy.

Factors	DF	Seq SS	Contribution (%)	Adj SS	Adj MS	*F*-value	*P*-value
CRP content	2	1028411	9.10	3646727	1823364	21.69	<0.001
NRL content	2	5884548	52.08	5884548	2942274	35.01	<0.001
TFH content	1	2023498	17.91	468942	468942	5.58	0.028
CRP Content*TFH content	2	663451	5.87	281557	140778	1.67	0.213
NRL Content*TFH content	2	18556	0.16	18556	9278	0.11	0.896
Error	20	1681041	14.88	1681041	84052		
Total	29	11299505	100.00				

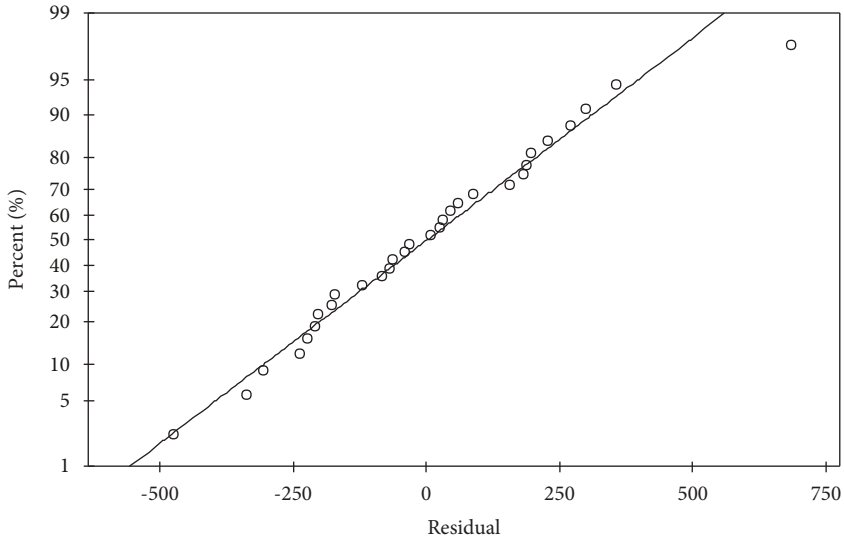

Figure 9: Normal probability plot of residual for fracture energy.

3.2. Fracture Resistance via Indirect Tensile Strength Test. The indirect tensile strength (ITS) test was conducted to determine the tensile properties of the asphalt mixtures based on the cracking characteristics of pavement. The ITS test is widely used to characterise the internal resistance of compacted asphalt mixtures. As one of the input factors in the asphalt pavement transverse cracking model utilised in the Pavement Mechanistic-Empirical (ME) Design Guide, the ITS test is a widely acknowledged test method [48]. Figure 10 shows the individual value plot of the asphalt mixture's tensile strength.

All the asphalt mixtures were tested at 15°C to measure the strength and stiffness of the entire asphalt mixture rather than the strength of the asphalt binder itself. At a higher temperature, such as 25°C, the testing will only induce stress on the layer of asphalt binder within the restrained asphalt mixture specimens rather than on the aggregates and asphalt binder. Figure 10 shows that the black circular point on each asphalt mixture type reflects the associated mean tensile strength value. Incorporating CRP and NRL modifiers in asphalt mixtures improves their tensile strength substantially. The mixture's volume increases when rubber modifiers are added to asphalt mixtures of all varieties. The tensile strength of the CRP-modified asphalt mixture increased by 17.32% and 32.40%, respectively, with the addition of 5% and 10% modifiers. The NRL-modified asphalt mixture increased by 17.88% with the 5% modifier and 30.17% with the 10% modifier.

Due to the higher tensile strength observed with the incorporation of TFH, it can be deduced that TFH facilitates enhancing the tensile strength of asphalt mixtures in this research. The addition of TFH into the control asphalt binder improved the tensile strength from 1.79 MPa to 1.99 MPa. In comparison, the CRP-modified asphalt mixture increased from 2.10 MPa to 2.26 MPa and from 2.37 MPa to 2.60 MPa for 5% and 10% modifier content, respectively. NRL-modified asphalt mixture with 5% modifier content rose from 2.11 MPa to 2.25 MPa and from 2.33 MPa to 2.52 MPa for 10% modified content with the incorporation of TFH. In addition, the increased indirect tensile strength suggests that the improved asphalt mixtures can withstand substantially bigger tensile strains before cracking or failing. Typically, asphalt mixtures with a low tensile strength are expected to break more than those with higher tensile strength. However, previous research has demonstrated that air voids in asphalt mixture, the aging process, moisture damage, and the freeze-thaw process also significantly influence the tensile strength of asphalt mixture and its service life [49].

The ITS of modified asphalt mixtures increases due to improved asphalt binder-aggregate adhesion, which enhances the toughness. Polymer efficiency on the ITS properties of asphalt mixtures is dependent on the asphalt source, polymer type, and polymer content [50–52]. In this case, the polymer type and polymer content are important in

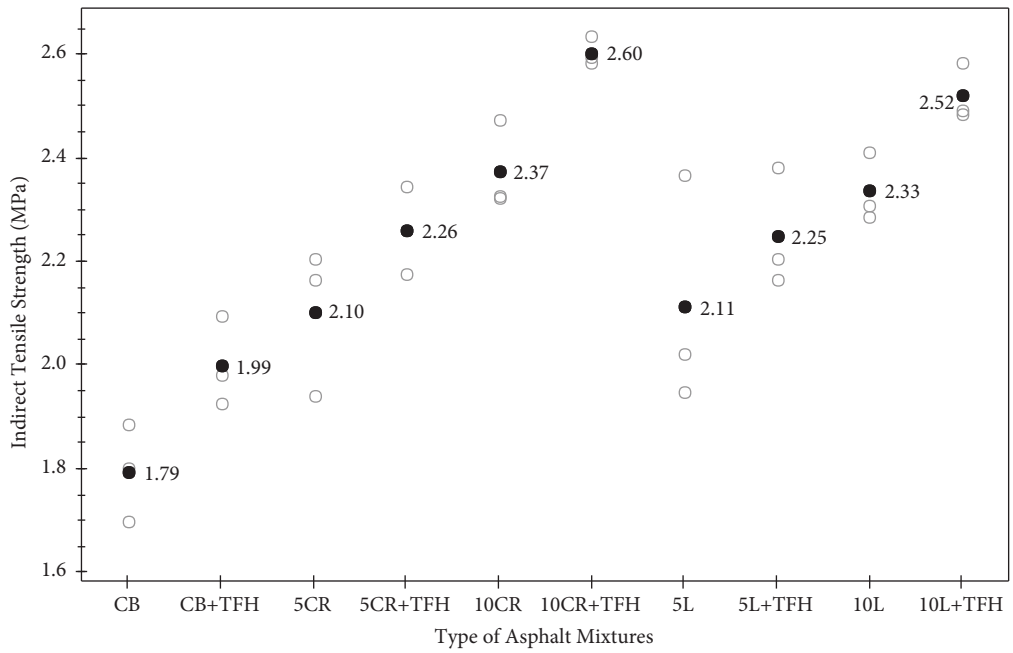

Figure 10: ITS of tested asphalt mixtures.

determining the tensile strength of the asphalt mixture. In comparison to plastomers, elastomers have a loosely cross-linked structure, which is responsible for their high tensile strength during chain stretching to a great extent [53, 54]. Therefore, the use of elastomer facilitated the improvement of the tensile strength of the asphalt mixture, and the addition of polymer content improved the tensile properties.

In addition to the influence of elastomers on tensile strength, the increased viscosity of the modified asphalt mixes contributed to the rise in indirect tensile strength. The increased viscosity is a result of the addition of rubber modifiers. Physical asphalt mixture hardening reflects an increase in stiffness. Also, the incorporation of TFH increased the asphalt binder's viscosity. The crystallisation of TFH wax was the additional element responsible for the physical hardening of the asphalt mixtures, which boosted their indirect tensile strength.

Theoretically, the rubber-modified asphalt binder experiences a glass transition state due to the changes in its mechanical, optical, and thermodynamic properties [55]. At this stage, the asphalt binder stiffens or hardens, which contributes to the asphalt mixture's strength. The time- and temperature-dependent viscoelastic behaviour of rubber-modified asphalt binders usually includes all four regions, namely, glassy, transition, plateau, and flow [56, 57]. The plateau is only possible if the asphalt binder has a polymeric network. However, the unmodified asphalt binder does not exhibit rubber-like behaviour, and their transition occurs directly from the glassy region to the flow region, with no glass transition stage or plateau region [58–60]. This might be the source of the control asphalt mixture's insufficient strength compared to the modified asphalt mixtures. The concept of the glass transition stage is applicable in this case, as it is widely used to research the rheological properties of the asphalt binder at below room temperature, which is the temperature adopted in this test. In conclusion, the addition of elastomer improves the resistance to cracking by enhancing the asphalt mixture's rheological and mechanical properties, especially its tensile strength.

3.2.1. Analysis of Variance of the Indirect Tensile Strength Test Results. The asphalt mixture's tensile strength increased due to the influence of modifier content and TFH, as measured by indirect tensile strength. Therefore, statistical analysis was carried out to determine the significance of the CRP modifier, NRL modifier, and TFH additives on the asphalt mixtures' performance. ANOVA was employed to formulate the effect of various factors on the indirect tensile strength of asphalt mixtures. Table 10 summarises the results of the analysis of variance using the general linear model. The effect of various factors on the stiffness properties of an asphalt mixture is considered significant if the P value is <0.05. In addition to evaluating the individual components, the effect of interaction between the modifier and the TFH additive was also evaluated.

As the P values were less than 0.05, the analysis of variance demonstrated that all individual factors were statistically significant and contributed to the tensile strength of asphalt mixtures. However, the interaction factors had no significant effect on the performance. The P values of the interaction factors were higher than 0.05. The percentage of contribution is based on the estimates of the variance components, indicating the degree of influence on the tensile strength properties. Therefore, as shown in Table 10, the NRL content accounted for 46.10% of the total variation in the measurements. The results showed that the addition of the NRL modifier at various percentages substantially increased the tensile strength properties compared to modified asphalt mixtures with CRP. The percentages of contribution

Table 10: ANOVA analysis of indirect tensile strength.

Factors	DF	Seq SS	Contribution (%)	Adj SS	Adj MS	F value	P value
CRP content	2	0.4839	26.37	1.0527	0.5264	42.82	<0.001
NRL content	2	0.8459	46.10	0.8458	0.4229	34.41	<0.001
TFH content	1	0.2511	13.68	0.0751	0.0752	6.12	0.022
CRP Content*TFH content	2	0.0044	0.24	0.0041	0.0021	0.17	0.847
NRL Content*TFH content	2	0.0037	0.20	0.0037	0.0019	0.15	0.860
Error	20	0.2458	13.40	0.2458	0.0123		
Total	29	1.8348	100				

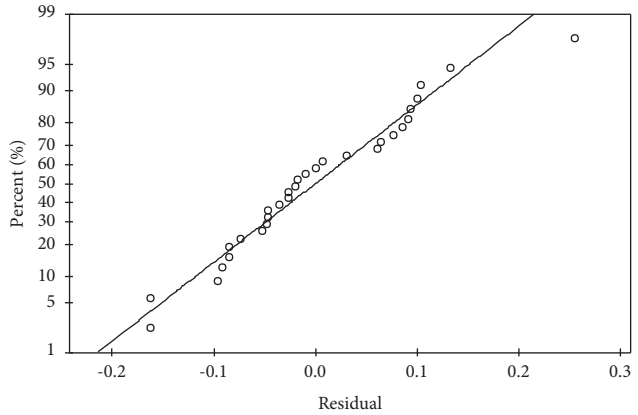

Figure 11: Normal probability plot of residual for ITS test.

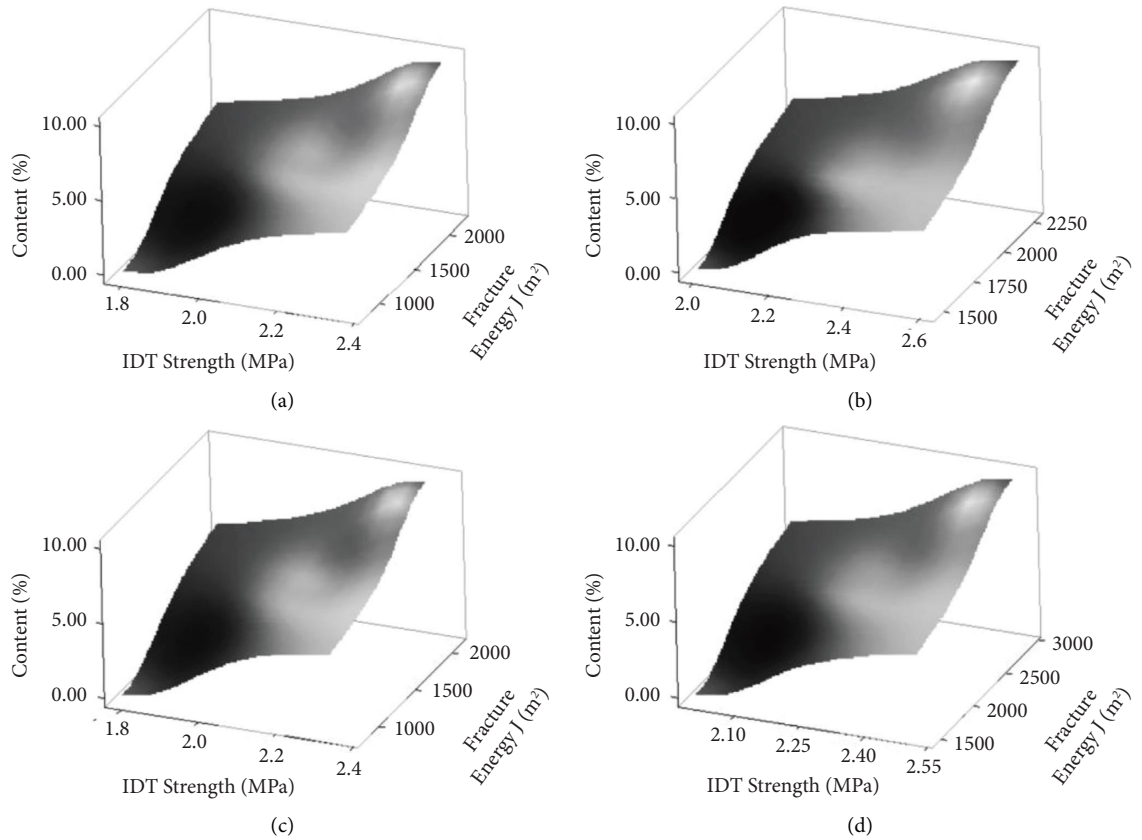

Figure 12: Correlations of asphalt mixture's ITS and fracture energy; (a) CRP without TFH, (b) CRP with TFH, (c) NRL without TFH, and (d) NRL with TFH.

for CRP content and TFH are 26.37% and 13.68%, respectively. Owing to the low contribution percentages of 0.24% and 0.20% for the CRP and NRL modifiers, respectively, the contribution due to the interaction between modifier content and TFH can be anticipated to be less significant. Figure 11 shows the normal plots of residuals. The normal probability plot of residuals reflects that the residuals have a normal distribution. The general linear model estimates the effects of various factors on the response of results based on the normal distribution of residuals. A normal probability plot of the residuals should follow a straight line.

3.3. Correlations between ITS and Fracture Energy of Asphalt Mixtures. This analysis shows a significant correlation between the ITS of the asphalt mixture and the asphalt mixture's fracture energy as determined by the SCB test. The ITS of asphalt mixture is commonly used to evaluate the potential cracking in compacted asphalt mixture. Meanwhile, the fracture energy represents the asphalt mixture's resistance to fracture. The ITS and fracture energy are interconnected with each other to secure good mechanical performance.

Figures 12(a)–12(d) show the 3D surface plot of the correlation. The analysis showed that ITS was directly proportional to the asphalt mixture's fracture energy, indicating a strong correlation relationship. The asphalt mixture's fracture energy increases as the ITS increases, which is attributed to the presence of rubber modifiers and a TFH additive. A higher ITS signifies that the asphalt mixture is resistant to cracking, and therefore, has greater fracture energy. Regardless of the presence of TFH, all types of asphalt mixture demonstrated similar attributes and tendencies. The correlation between the results of the ITS test and those of the SCB test indicated that the SCB test's findings are plausible.

4. Conclusions

The synergistic outcomes of adding CRP, NRL, and synthetic wax to the asphalt mixtures' fracture energy and fracture resistance characteristics were evaluated based on SCB and ITS tests. The 3D plots clearly showed that the higher CRP and NRL improved cracking resistance. In addition, the fracture energy was improved by 1.75–3.75 times, depending on the use of TFH, CRP, and NRL content. Notably, the mixture with 10% NRL and TFH had the highest fracture energy. A similar pattern was discovered for fracture toughness and stiffness.

Although higher fracture energy and cracking resistance are positive aspects, they might have an adverse effect on the other aspects. Analysis of V_{FI} and V_{CG} showed that the incorporation of CRP and TFH improved crack propagation speed as a result of the stiffness of the binder, which made the mixture more brittle in contrast to the control mix. Statistical analysis through a general linear model showed that the modifier (CRP and NRL) contents significantly affect the fracture energy. In addition, the model outputs showed that the percentages of contributions for CRP content and TFH additive in terms of crack resistance property were 9.10% and 17.91%, respectively, while the contribution due to the interaction between modifier content and TFH additive was less significant. Furthermore, the fracture energy, fracture toughness, and indirect tensile strength of mixtures containing 5% NRL were comparable with those containing 5% CRP (with or without TFH), while the mixtures containing 10% NRL showed higher fracture energy and stiffness than their counterpart mixtures with 10% CRP. As a result, the selection of the rubber type is a critical criterion for the fracture properties of rubber-modified mixtures.

All modified binder samples exhibit a direct correlation between the fracture energy determined by the SCB test and the cracking resistance shown by the ITS test. Changes in fracture energy and crack resistance can be attributed to different chemical structures and crystallisation processes, material sources, and binder additives. In conclusion, the interaction of CRP or NRL with TFH improves the structural adequacy of asphalt mixtures. However, the appropriate percentage of each material should be selected for better performance.

Data Availability

The data used to support the findings of this research are included within the article.

Conflicts of Interest

The authors declare that they have no conflicts of interest.

Acknowledgments

The authors sincerely acknowledge the Ministry of Higher Education Malaysia for the Fundamental Research Grant Scheme with Project Code: FRGS/1/2021/TK01/USM/02/1 that enabled us to conduct this research work. Support from Universiti Sains Malaysia via a Research University Individual (RUI) Grant (1001.PAWAM.8014140) is also appreciated. A special thanks to material suppliers for extending their support. The authors also express their appreciation to the technicians of the Highway Engineering Laboratory and Materials Engineering Laboratory at Universiti Sains Malaysia for their help.

References

[1] J. W. Chew, S. Poovaneshvaran, M. R. Mohd Hasan, H. Wang, A. Sani, and B. Golchin, "Serviceability during asphaltic concrete production and leaching concerns of asphalt mixture prepared with recycled paper mill sludge," *International Journal of Pavement Engineering*, vol. 23, no. 2, pp. 137–147, 2022.

[2] A. Sani, M. R. Mohd Hasan, K. A. Shariff, A. Jamshidi, A. H. Ibrahim, and S. Poovaneshvaran, "Engineering and microscopic characteristics of natural rubber latex modified binders incorporating silane additive," *International Journal of Pavement Engineering*, vol. 21, no. 14, pp. 1874–1883, 2020.

[3] H. Wang, X. Liu, M. van de Ven, G. Lu, S. Erkens, and A. Skarpas, "Fatigue performance of long-term aged crumb rubber modified bitumen containing warm-mix additives," *Construction and Building Materials*, vol. 239, Article ID 117824, 2020.

[4] K. Yan, S. Wang, D. Ge, J. Chen, S. Tian, and H. Sun, "Laboratory performance of asphalt mixture with waste tyre rubber and APAO modified asphalt binder," *International Journal of Pavement Engineering*, vol. 23, no. 1, pp. 59–69, 2022.

[5] T. A. Balqis and S. Suherman, "The effect of using crumb rubber on fatigue and rutting lives in flexible pavement," *IOP Conference Series: Materials Science and Engineering*, vol. 732, no. 1, Article ID 12030, 2020.

[6] J. H. Liu, "Fatigue life evaluation of asphalt rubber mixtures using Semi-Circular Bending test," *Advanced Materials Research*, vol. 260, pp. 3444–3449, 2011.

[7] T. Ma, H. Wang, L. He, Y. Zhao, X. Huang, and J. Chen, "Property characterization of asphalt binders and mixtures modified by different crumb rubbers," *Journal of Materials in Civil Engineering*, vol. 29, no. 7, 2017.

[8] A. Ameli, R. Babagoli, M. Khabooshani, R. AliAsgari, and F. Jalali, "Permanent deformation performance of binders and stone mastic asphalt mixtures modified by SBS/montmorillonite nanocomposite," *Construction and Building Materials*, vol. 239, Article ID 117700, 2020.

[9] C. Yan, W. Huang, M. Zheng, Y. Zhang, and P. Lin, "Influence of ageing on high content polymer modified asphalt mixture stripping, cracking and rutting performances," *Road Materials and Pavement Design*, vol. 22, no. 8, pp. 1824–1841, 2021.

[10] M. Marasteanu, A. Zofka, M. Turos et al., *Investigation of Low Temperature Cracking in Asphalt Pavements A Transportation Pooled Fund Study*, Report No,: MN/RC 2007-43, pp. 81655–82128, Minnesota Department of Transportation, St paul, MN, USA, 2007.

[11] M. Diakhaté, A. Millien, C. Petit, A. Phelipot-Mardelé, and B. Pouteau, "Experimental investigation of tack coat fatigue performance: towards an improved lifetime assessment of pavement structure interfaces," *Construction and Building Materials*, vol. 25, no. 2, pp. 1123–1133, 2011.

[12] X. Qiu, J. Xu, W. Xu, S. Xiao, F. Wang, and J. Yuan, "Characterization of fatigue damage mechanism of asphalt mixtures with acoustic emission," *Construction and Building Materials*, vol. 240, Article ID 117961, 2020.

[13] S. Benaboud, M. Takarli, B. Pouteau et al., "Fatigue damage monitoring and analysis of aged asphalt concrete using acoustic emission technique," *Road Materials and Pavement Design*, vol. 22, no. 1, pp. S592–S603, 2021.

[14] A. T. Zehnder, "Modes of fracture," in *Encyclopedia of Tribology*, Q. J. Wang and Y.-W. Chung, Eds., pp. 2292–2295, Springer US, Boston, MA, USA, 2013.

[15] T. H. G. Megson, "Properties of engineering materials," *Structural and Stress Analysis*, pp. 184–208, Elsevier, Netherlands, Europe, 2014.

[16] R. Roque, B. Birgisson, B. Sangpetngam, and Z. Zhang, "Hot mix asphalt fracture mechanics: a fundamental crack growth law for asphalt mixtures," *Asphalt Paving Technology: Association of Asphalt Paving Technologists*, vol. 71, pp. 816–827, 2002.

[17] H. Wei, J. Li, F. Wang, J. Zheng, Y. Tao, and Y. Zhang, "Numerical investigation on fracture evolution of asphalt mixture compared with acoustic emission," *International Journal of Pavement Engineering*, vol. 23, no. 10, pp. 3481–3491, 2021.

[18] A. Jamshidi, G. White, and K. Kurumisawa, "Rheological characteristics of epoxy asphalt binders and engineering properties of epoxy asphalt mixtures–state-of-the-art," *Road Materials and Pavement Design*, vol. 23, 2021.

[19] J. He, L. Liu, H. Yang, M. R. M. Aliha, and H. R. Karimi, "Contribution of interface fracture mechanism on fracture propagation trajectory of heterogeneous asphalt composites contribution of interface fracture mechanism on fracture propagation," *Applied Sciences*, vol. 11, 2021.

[20] A. Braham, W. Buttlar, and F. Ni, "Laboratory mixed-mode cracking of asphalt concrete using the single-edge notch beam," *Road Materials and Pavement Design*, vol. 11, no. 4, pp. 947–968, 2010.

[21] W. Xu, X. Wei, J. Wei, and Z. Chen, "Experimental evaluation of the influence of aggregate strength on the flexural cracking behavior of epoxy asphalt mixtures," *Materials*, vol. 13, no. 8, p. 1876, 2020.

[22] M. P. Wagoner, W. G. Buttlar, G. H. Paulino et al., "Investigation of the fracture resistance of hot-mix asphalt concrete using a disk-shaped compact tension test," *Transportation Research Record: Journal of the Transportation Research Board*, vol. 1929, 2005.

[23] H. Kim, M. P. Wagoner, and W. G. Buttlar, "Micromechanical fracture modeling of asphalt concrete using a single-edge notched beam test," *Materials and Structures*, vol. 42, no. 5, pp. 677–689, 2009.

[24] M. R. M. Aliha, H. Fazaeli, S. Aghajani, and F. Moghadas Nejad, "Effect of temperature and air void on mixed mode fracture toughness of modified asphalt mixtures," *Construction and Building Materials*, vol. 95, pp. 545–555, 2015b.

[25] X. Li, A. F. Braham, M. O. Marasteanu, W. G. Buttlar, and R. C. Williams, "Effect of factors affecting fracture energy of asphalt concrete at low temperature," *Road Materials and Pavement Design*, vol. 9, no. 1, pp. 397–416, 2008.

[26] C. M. Stewart, C. W. Oputa, and E. Garcia, "Effect of specimen thickness on the fracture resistance of hot mix asphalt in the disk-shaped compact tension (DCT) configuration," *Construction and Building Materials*, vol. 160, pp. 487–496, 2018.

[27] M. R. M. Aliha, H. Behbahani, H. Fazaeli, and M. H. Rezaifar, "Study of characteristic specification on mixed mode fracture toughness of asphalt mixtures," *Construction and Building Materials*, vol. 54, pp. 623–635, 2014.

[28] H. Wang, C. Zhang, L. Li, Z. You, and A. Diab, "Characterization of low temperature crack resistance of crumb rubber modified asphalt mixtures using semi-circular bending tests," *Journal of Testing and Evaluation*, vol. 44, no. 2, Article ID 20150145, 2016.

[29] M. M. Mirsayar, X. Shi, and D. G. Zollinger, "Evaluation of interfacial bond strength between Portland cement concrete and asphalt concrete layers using bi-material SCB test specimen," *Engineering Solid Mechanics*, vol. 5, no. 4, pp. 293–306, 2017.

[30] M. Mubaraki, A. A. Abd-Elhady, H. El-Din, and M. Sallam, "Mixed mode fracture toughness of recycled tire rubber-filled concrete for airfield rigid pavements," *International Journal of Pavement Research and Technology*, vol. 6, 2013.

[31] M. R. M. Aliha, M. J. Sarbijan, and A. Bahmani, "Fracture toughness determination of modified HMA mixtures with two novel disc shape configurations," *Construction and Building Materials*, vol. 155, pp. 789–799, 2017.

[32] A. Bahmani, F. Farahmand, F. Ataei, and M. R. M. Aliha, "Mixed mode I/III fracture parameters for edge-notched diametrically compressed disc specimen," *Material Design & Processing Communications*, vol. 1, no. 6, 2019.

[33] M. R. M. Aliha, A. Bahmani, and S. Akhondi, "Determination of mode III fracture toughness for different materials using a new designed test configuration," *Materials and Design*, vol. 86, pp. 863–871, 2015a.

[34] S. Najjar, A. Mohammadzadeh Moghaddam, A. Sahaf, and M. R. M. Aliha, "Low temperature fracture resistance of cement emulsified asphalt mortar under mixed mode I/III loading," *Theoretical and Applied Fracture Mechanics*, vol. 110, Article ID 102800, 2020.

[35] K. Elias Kaloush, K. Prapoorna Biligiri, W. Abdelaziz Zeiada, M. Carolina Rodezno, and J. Xavier Reed, "Evaluation of fiber-reinforced asphalt mixtures using advanced material characterization tests," *ASTM International*, vol. 38, 2010.

[36] Z. Zhang, R. Roque, and B. Birgisson, "Evaluation of laboratory-measured crack growth rate for asphalt mixtures," *Transportation Research Record*, vol. 1767, 2001.

[37] S. R. Omranian, M. O. Hamzah, and M. R. M. Hasan, "Introducing new indicators to evaluate fracture properties of asphalt mixtures using semicircular bending test," *Iranian Journal of Science and Technology - Transactions of Civil Engineering*, vol. 43, no. 3, pp. 541–549, 2019.

[38] S. R. Omranian, M. O. Hamzah, T. S. Yee, and M. R. Mohd Hasan, "Effects of short-term ageing scenarios on asphalt mixtures' fracture properties using imaging technique and response surface method," *International Journal of Pavement Engineering*, vol. 21, no. 11, pp. 1374–1392, 2020.

[39] D. Yang, H. R. Karimi, and M. R. M. Aliha, "Comparison of testing method effects on cracking resistance of asphalt concrete mixtures," *Applied Sciences (Switzerland)*, vol. 11, no. 11, p. 5094, 2021.

[40] M. R. Mohd Hasan, B. W. Colbert, Z. You et al., "A review on utilization of electronic waste plastics for use within asphaltic concrete materials: development, opportunities and challenges for successful implementation," *Encyclopedia of Renewable and Sustainable Materials*, Elsevier, Netherlands, Europe, 2020.

[41] N. Sabahfar, A. Ahmed, S. R. Aziz, and M. Hossain, "Cracking resistance evaluation of mixtures with high percentages of reclaimed asphalt pavement," *Journal of Materials in Civil Engineering*, vol. 29, no. 4, Article ID 6016022, 2017.

[42] M. Zarei, A. Abdi Kordani, and M. Zahedi, "Evaluation of fracture behavior of modified Warm Mix Asphalt (WMA) under modes I and II at low and intermediate temperatures," *Theoretical and Applied Fracture Mechanics*, vol. 114, Article ID 103015, 2021.

[43] A. Kavussi and S. M. Motevalizadeh, "Fracture and mechanical properties of water-based foam warm mix asphalt containing reclaimed asphalt pavement," *Construction and Building Materials*, vol. 269, Article ID 121332, 2021.

[44] A. A. Yousefi, S. Sobhi, M. R. M. Aliha, S. Pirmohammad, and H. F. Haghshenas, "Cracking properties of warm mix asphalts containing reclaimed asphalt pavement and recycling agents under different loading modes," *Construction and Building Materials*, vol. 300, Article ID 124130, 2021.

[45] D. Liu and D. J. Pons, "Crack propagation mechanisms for creep fatigue: a consolidated explanation of fundamental behaviours from initiation to failure," *Metals*, vol. 8, no. 8, p. 623, 2018.

[46] G. Saha and K. P. Biligiri, "Fracture damage evaluation of asphalt mixtures using Semi-Circular Bending test based on fracture energy approach," *Engineering Fracture Mechanics*, vol. 142, pp. 154–169, 2015.

[47] P. Rath, N. Gettu, S. Chen, and W. G. Buttlar, "Investigation of cracking mechanisms in rubber-modified asphalt through fracture testing of mastic specimens," *Road Materials and Pavement Design*, vol. 23, no. 7, pp. 1544–1563, 2021.

[48] American Association of State Highway and Transportation Officials, *Mechanistic-empirical Pavement Design Guide: A Manual of Practice*, American Association of State Highway and Transportation Officials, Washington, D.C, USA, 2008.

[49] M. R. Islam, M. I. Hossain, and R. A. Tarefder, "A study of asphalt aging using Indirect Tensile Strength test," *Construction and Building Materials*, vol. 95, pp. 218–223, 2015.

[50] A. Behnood, A. Shah, R. S. McDaniel, M. Beeson, and J. Olek, "High-temperature properties of asphalt binders: comparison of multiple stress creep recovery and performance grading systems," *Transportation Research Record*, vol. 2574, no. 1, pp. 131–143, 2016.

[51] A. Behnood and J. Olek, "Rheological properties of asphalt binders modified with styrene-butadiene-styrene (SBS), ground tire rubber (GTR), or polyphosphoric acid (PPA)," *Construction and Building Materials*, vol. 151, pp. 464–478, 2017a.

[52] A. Behnood and J. Olek, "Stress-dependent behavior and rutting resistance of modified asphalt binders: an MSCR approach," *Construction and Building Materials*, vol. 157, pp. 635–646, 2017b.

[53] K. Gopalakrishnan, J. van Leeuwen, Hans), and R. C. Brown, "Sustainable bioenergy and bioproducts: value added engineering applications 001," *Green Energy and Technology*, vol. 62, 2012.

[54] V. R. Sastri, *Plastics in Medical Devices: Properties, Requirements, and Applications*, William Andrew Publishing: Oxford, New York, NY, USA, 2013.

[55] P. Kriz, J. Stastna, and L. Zanzotto, "Glass transition and phase stability in asphalt binders," *Road Materials and Pavement Design*, vol. 9, no. 1, pp. 37–65, 2008.

[56] B. Singh, M. Gupta, and H. Tarannum, "Mastic of polymer-modified bitumen and poly(vinyl chloride) wastes," *Journal of Applied polymer science*, vol. 140, 2003.

[57] S. Senise, V. Carrera, A. A. Cuadri, F. J. Navarro, and P. Partal, "Hybrid rubberised bitumen from reactive and non-reactive ethylene copolymers," *Polymers*, vol. 11, no. 12, p. 1974, 2019.

[58] A. H. Fawcett and T. McNally, "Polystyrene and asphaltene micelles within blends with a bitumen of an SBS block copolymer and styrene and butadiene homopolymers," *Colloid and Polymer Science*, vol. 281, no. 3, pp. 203–213, 2003.

[59] C. Fuentes-Audén, F. J. Martínez-Boza, F. J. Navarro, P. Partal, and C. Gallegos, "Formulation of new synthetic binders: thermo-mechanical properties of recycled polymer/oil blends," *Polymer Testing*, vol. 26, no. 3, pp. 323–332, 2007.

[60] S. Dessouky, C. Reyes, M. Ilias, D. Contreras, and A. T. Papagiannakis, "Effect of pre-heating duration and temperature conditioning on the rheological properties of bitumen," *Construction and Building Materials*, vol. 25, no. 6, pp. 2785–2792, 2011.